

# Comparing Virtual Reality to Conventional Simulator Visuals: Effects of Peripheral Visual Cues in Roll-Axis Tracking Tasks

Lorenzo Terenzi\* and Peter M. T. Zaal†

*San José State University*

*NASA Ames Research Center*

*Moffett Field, CA 94035*

This paper compares the effects of peripheral visual cues on manual control between a conventional fixed-base simulator and virtual reality. The results were also compared with those from a previous experiment conducted in a motion-base simulator. Fifteen participants controlled a system with second-order dynamics in a disturbance-rejection task. Tracking performance, control activity, simulator sickness questionnaire answers, and biometrics were collected. Manual control behavior was modeled for the first time in a virtual reality environment. Virtual reality did not degrade participants' manual control performance or alter their control behavior. However, peripheral cues were significantly more effective in virtual reality. Control activity decreased for all conditions with peripheral cues. The trends introduced by the peripheral visual cues from the previous experiment were replicated. Finally, VR was not more nauseogenic than the conventional simulator. These results suggest that virtual reality might be a good alternative to conventional fixed-base simulators for training manual control skills.

## I. Nomenclature

$A_i$	=	Amplitude of the $i^{\text{th}}$ sine of the disturbance signal, deg
$e$	=	Roll attitude error, rad
$f_d$	=	Disturbance forcing function, $\text{rad s}^{-1}$
$H_c$	=	Controlled dynamics transfer function
$H_p$	=	Human operator transfer function
$K_p$	=	Human operator gain, –
$n$	=	Remnant signal, rad
$RMS_e$	=	Root mean square of the roll error, deg
$RMS_u$	=	Root mean square of the control input, deg
$s$	=	Laplace variable
$T_l$	=	Human operator lead time constant, s
$t$	=	Time, s
$VAF$	=	Variance accounted for, %
$\zeta_{nm}$	=	Human operator neuromuscular damping, –
$\tau$	=	Human operator time delay, s
$\phi$	=	Roll attitude, rad
$\phi_i$	=	Phase of the $i^{\text{th}}$ sine of the disturbance signal, rad
$\varphi_m$	=	Phase margin, deg
$\omega$	=	Frequency, $\text{rad s}^{-1}$
$\omega_{nm}$	=	Human operator neuromuscular frequency, $\text{rad s}^{-1}$
$\omega_c$	=	Crossover frequency, $\text{rad s}^{-1}$
$\omega_i$	=	Frequency of the $i^{\text{th}}$ sine of the disturbance signal, $\text{rad s}^{-1}$

\*Research Scholar, Human Systems Integration Division, Mail Stop 262-2, lorenzo.terenzi@nasa.gov, Student Member.

†Senior Research Engineer, Human Systems Integration Division, Mail Stop 262-2, peter.m.t.zaal@nasa.gov, Senior Member.

## II. Introduction

THIS paper investigates the effects of peripheral visual cues on manual control behavior in a roll-axis tracking task using virtual reality (VR) and conventional simulator visuals. With the rapidly increasing need for new pilots, both in commercial and military aviation now and in new domains such as urban air mobility in the future, and the increasing need for compact in-mission training devices, novel training solutions are required. Head-mounted displays (HMDs) could facilitate these novel training solutions as they are a compact and cost-effective alternative to the large simulator visual systems currently used in most training devices. Recent advances in HMD technologies make VR more suitable for scientific and commercial purposes [1]. However, limited research has been performed comparing human behavior and performance between VR and conventional simulator visuals, which is important to understand the validity of VR technology for training.

Peripheral visual cues have shown to increase human manual control performance in manual control tasks. In particular, they have a similar effect on performance and control behavior compared to motion cues [2–5]. VR is particularly promising in this regard, since the high level of immersion in virtual environments reported by most users can aid to increase the effectiveness of peripheral visual cues.

This study provides data to help determine the feasibility of using VR for the training of manual control skills by comparing manual control behavior and performance between VR and typical simulator visuals. In addition, motion or cybersickness was evaluated in both simulation environments. Pilots had to perform a roll disturbance-rejection task with and without the presence of peripheral visual cues. Manual control behavior was identified using a cybernetic approach. This approach has been used in many studies in the past [3–7]; however, never in a VR environment. The basic setup of the experiment was replicated from the experiments conducted by Hosman and Van der Vaart [4], and, successively, by Pool et al. [5]. This allowed for validation of the conventional simulator visuals, the baseline.

## III. Methodology

This study used a roll disturbance-rejection task, which required participants to actively minimize the error shown on a compensatory display by providing lateral manual control inputs. This task was chosen for two reasons: firstly, it resembles many manual control tasks that pilots face in an aircraft, like following a glideslope during landing or keeping an aircraft level under turbulence, and, secondly, it was used in the past by Pool et al. and Hosman and Van Der Vaart [3, 5] in experiments that investigated the effects of peripheral visual and physical motion cues on manual control behavior.

### A. Control Task

Participants performed a roll disturbance-rejection task. Fig. 1 depicts the block diagram of the task. Participants minimized the error  $e$  on a compensatory display while controlling the controlled roll dynamics which were disturbed by a disturbance forcing function  $f_d$ . The participants had to continuously compensate for the disturbances with control inputs  $u$ . The task was performed in both a VR environment and a fixed-base simulator and with and without peripheral visual cues provided by a checkerboard pattern (Sec. IV).

The controlled dynamics used in the roll control task resembled double-integrator dynamics:

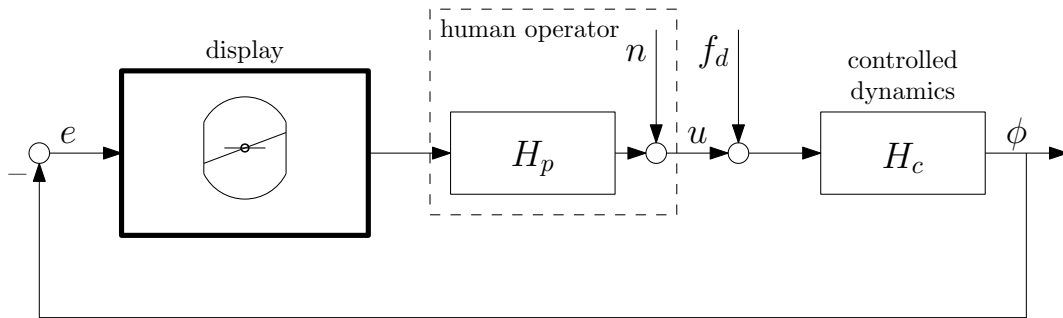


Fig. 1 Control task block diagram.

$$H_c = \frac{4}{s^2} \quad (1)$$

In the control task in Fig. 1 with the double-integrator dynamics of Eq. 1, human operators' manual control behavior can be described by a linear transfer function with five parameters:

$$H_p = K_p(T_L s + 1)e^{-s\tau} \frac{\omega_{nm}^2}{s^2 + 2\zeta_{nm}\omega_{nm}s + \omega_{nm}^2} \quad (2)$$

where  $K_p$  is the human-operator gain,  $T_L$  is the lead-time constant,  $\tau$  is the human processing delay,  $\omega_{nm}$  is the neuromuscular frequency, and  $\zeta_{nm}$  is the neuromuscular damping ratio. The term  $k_p(T_L s + 1)$  represents a proportional-derivative (PD) controller which is necessary to control the second-order system. The term  $e^{-s\tau}$  represents the delay due to the information processing that humans experience between perceiving an input and responding to it. Finally, the term  $\frac{\omega_{nm}^2}{s^2 + 2\zeta_{nm}\omega_{nm}s + \omega_{nm}^2}$  represents a second-order spring-damper system, which captures the dynamics of the human actuation system. The difference between the output of the linear transfer function  $H_p$  and the measured control signal  $u$  is the remnant signal  $n$  which accounts for nonlinear behavior and noise (Fig. 1).

The disturbance function  $f_d$ , the same as the one chosen by Hosman and Van Der Vaart, was a linear combination of ten sine waves with different frequencies, amplitudes, and phases:

$$f_d(t) = \sum_{i=1}^{10} A_i \sin(\omega_i t + \phi_i) \quad (3)$$

where  $A_i$  is the amplitude of the  $i^{\text{th}}$  sine wave,  $\phi_i$  the phase, and  $\omega_i$  the frequency. The exact value of amplitudes, phases and frequencies can be found in McRuer et al. [8]. The disturbance forcing function amplitudes were pre-filtered by the inverse controlled dynamics  $H_c^{-1}$  to ensure its spectrum was not affected by the controlled system.

## B. Previous Studies

The effects of motion and visual peripheral cues on manual control have been investigated in the past [2–5]. Hosman and Van Der Vaart performed an experiment on a motion-base simulator where participants had to perform both target-following and disturbance-rejection tasks. In the target-following task the objective was to follow a target roll signal, while for the disturbance-rejection task the objective was to counteract roll disturbances applied to the controlled system. They found a consistent improvement in performance with the addition of peripheral visual cues to the central compensatory display [4].

Pool et al. replicated and extended their experiment on a six-degree-of-freedom motion simulator. In this experiment participants had to perform two tasks of different difficulty under the different experimental conditions tested by Hosman and Van Der Vaart. This study confirmed most of the previous findings and discovered a decrease in effectiveness of peripheral visual cues in the easier target-following task [5]. The current study utilized the disturbance-rejection task used by Hosman and Van Der Vaart and Pool et al. and replicated two experimental conditions to verify some of their results and create a baseline for comparing the current results in VR.

# IV. Experiment Setup

## A. Independent Variables

The experiment had two independent variables: simulation environment with two levels (fixed-base simulator or VR) and visual cues with three levels (central display only (C), central display with peripheral cues (CP), and central display with peripheral cues in the far peripheral visual field (CPHF)). A  $2 \times 2$  full-factorial design, without using the CPHF condition, was used to generate the test matrix. The CPHF condition was only tested in the fixed-base simulator. The test matrix with multiple repetitions of the five experimental conditions was ordered following the Latin square design to ensure ordering effects were reduced. The experiment had a repeated-measures design.

The compensatory display was used in all experimental conditions. The display was depicted on a separate physical display in the fixed-base simulator or rendered in the 3D virtual environment. For the CP and CPHF conditions, high-contrast checkerboard patterns were rendered either on the out-the-window visual system of the fixed-base simulator



**Fig. 2 Fixed-base simulator setup and VR equipment.**

or in the same physical location in VR. The checkerboard pattern moved in sync with the aircraft roll attitude [4]. This means the checkerboard also moved in sync with the error on the compensatory display (Fig. 1).

In the fixed-base simulator setup, a third visual condition was tested: CPHF. This condition imitated the geometry of the original experiments of Hosman and Van Der Vaart and Pool et al. exactly. This condition could not be tested in VR due to the limited field of view of the currently available headsets. Note that of the five experimental conditions, only two were replications from the previous experiments: C and CPHF in the fixed-base simulator.

## **B. Apparatus**

Both a conventional fixed-base simulator setup and an HMD with base stations were used. The fixed-based simulator is a research simulator located at NASA Ames Research Center. The simulator has a collimated out-the-window visual system with a field of view of 210 degrees. Three different projectors, all driven by a separate computer, each rendered approximately 70 degrees of the scene. Only the outer two projectors were used for the experiment. The central projector remained switched off. The simulator has a central seat with a Thrustmaster Hotas Warthog joystick on the right side to provide control inputs. For the VR conditions, an HTC Vive Pro headset was used as the HMD. Participants were seated in the exact same location using the same joystick while using the HMD. Two base stations tracked the location and orientation of the headset in 3D space. The simulator setup is depicted in Fig. 2.

Figs. 3 and 4 show the compensatory display and the checkerboard pattern used to generate peripheral visual cues, respectively. No other visual cues were provided. The geometry used to generate peripheral visual cues in the CP and CPHF conditions is shown in Fig. 5a and Fig. 5b, respectively. Note that the checkerboards in CP were symmetric and extended more forward compared to in CPHF. The checkerboards in CPHF were not symmetric and mimicked the participant sitting closer to the checkerboard on the right side (or sitting in the right seat of a cockpit with two seats) as in the experiments of Hosman and Van Der Vaart and Pool et al.

Biometrics were collected with the MindWare Mobile Impedance Cardiograph.

## **C. Participants**

Fifteen subjects participated in the experiment. Since fundamental questions about human control behavior were investigated, participants were not required to have flight experience. Participants, 11 males and 4 females, had a median age of 24 years ( $IQR = 23-27$ ). Their experience with VR and simulators (low = 1-10 h, medium = 10-50 h, and high = 50+ h), and flying (low = 1-50 h, medium = 50-250 h, and high = 250+ h), is summarized in Table 1. This table also

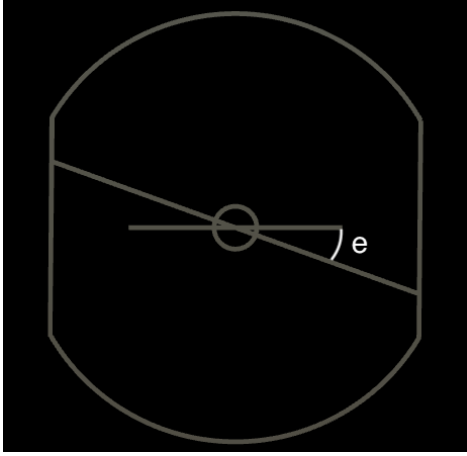


**Fig. 3 Compensatory display.**

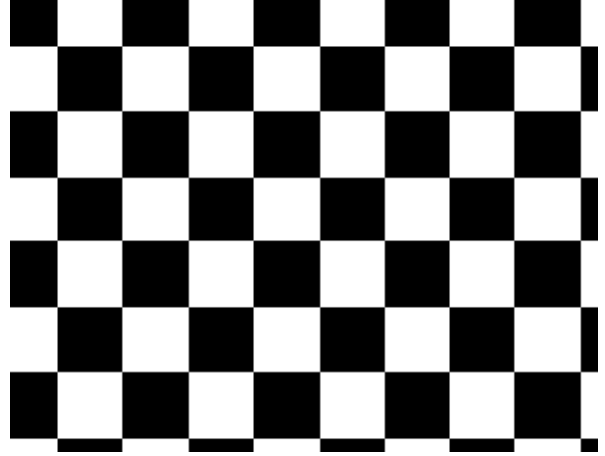


**Fig. 4 Checkerboard pattern used to generate peripheral visual motion cues.**

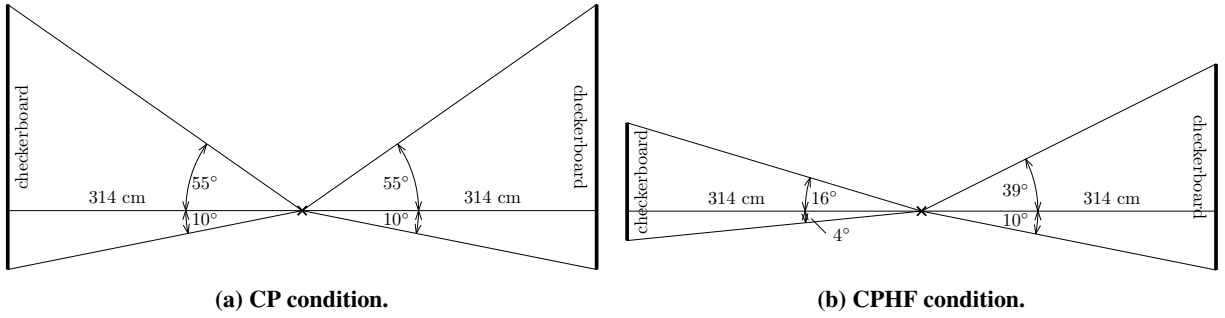


**Fig. 5 Geometry used to generate peripheral visual cues.**

provides participants' self-assessed propensity to motion sickness as determined by passed experiences.

**Table 1 Participant experience and motion sickness propensity.**

	Number of Participants			
	None	Low	Medium	High
VR Experience	8	7	0	0
Flying Experience	12	2	1	0
Simulator Experience	8	2	5	0
Motion Sickness Propensity	3	9	3	0

#### D. Procedures

Participants were given an extensive briefing about the experiment and the control task. They were told that the goal of the experiment was to evaluate the technology readiness level of VR headsets for the training of manual control tasks. Participant were encouraged to provide continuous control inputs and to always try to counteract any disturbances. After the briefing, the participants put on the sensors necessary to gather skin conductivity and electrocardiogram data. Before starting the experiment, they also completed a demographics questionnaire and simulator sickness questionnaire (SSQ) to assess their baseline level of well-being [9]. The initial SSQ scores were subtracted from the SSQ scores measured during the experiment.

The participants alternated experiencing either the fixed-base simulator or VR first to balance learning effects. The

participants started with a familiarization phase. This phase usually lasted a few runs and it ended when the participant was able to stabilize the system. The experiment continued with a training phase of nine runs for the fixed-base simulator or eight runs for VR. Occasionally, more training runs were required when participants did not reach asymptotic performance after the pre-determined number of training runs; that is, if they were still learning and improving. For each of the five experimental conditions, five measurement runs were recorded. Each run lasted 92 s, of which only 81.92 s were used to calculate the results of the experiment. The first 8.08 s and the last 2 seconds of the run were excluded.

After completing the task in the first simulator setup, the participants took a break of 15 minutes. During the break, they filled out another SSQ. After the break participants were trained for a minimum of six more runs on the second simulator setup or until asymptotic performance was reached. After training, the second set of measurements was taken. At the end of the experiment, participants again filled out the SSQ.

## E. Dependent Measures

The following dependent measures were collected:

- Simulator sickness questionnaire (SSQ) scores [9].
- The root mean square (RMS) of the error signal  $RMS_e$ , a measure of tracking performance. A lower  $RMS_e$  means better performance.
- The RMS of the control signal  $RMS_u$ , a measure of control activity. A higher  $RMS_u$  means a higher control activity.
- Five human-operator model parameters:  $K_p$ ,  $T_l$ ,  $\tau$ ,  $\omega_{nm}$ , and  $\zeta_{nm}$ . These parameters characterize human manual control behavior and were estimated using maximum likelihood estimation (MLE) [10].
- Biometrics: skin conductivity and heart rate. Higher skin conductivity and heart rate are associated with motion sickness.

## F. Hypotheses

The following hypotheses were formulated:

- H1*: Participants were expected to have a lower  $RMS_e$  and higher  $RMS_u$  in the fixed-base simulator compared to VR. The resolution and field of view of the HMD were lower compared to the fixed-base simulator and some artifacts, such as the screen-door effect or image distortion, were present.
- H2*: Participants were expected to have a lower  $RMS_e$  and  $RMS_u$  in the CP compared to the C condition as the presence of the moving peripheral visual cues was expected help with controlling the dynamical system.
- H3*: In the CP conditions, the lead constant  $T_l$  was hypothesized to be higher compared to the that in the C conditions.
- H4*: We expected a strong interaction effect between the visual condition and the simulator setup. VR is immersive and the presence of visual cues was expected to have a higher impact compared to conventional simulator visuals.
- H5*: We expected the SSQ scores for VR to be higher than those of the conventional simulator.
- H6*: Dependent measures were expected to not be significantly different between the CP and the CPHF conditions as in both cases, the peripheral visual cues were placed relatively far in the peripheral vision of the observer.

## V. Results

In this section, the experimental results, and the associated statistical tests, are presented. Of the 15 subjects who participated in the experiment, data from only 12 was used. One participant's performance was considered an outlier since the  $RMS_e$  was consistently more than three standard deviations from the group mean. Two other participants were excluded because they reported tiredness and frustration during the experiment. Their control errors (such as control inversions or loss of control) became very frequent over the course of the experiment, resulting in higher and more fluctuating  $RMS_e$  values. This made a significant part of their runs unusable.

Tables 2 and 3 summarize the means and standard deviations of the dependent measures for each condition. subsection V.A further presents the task performance results, subsection V.B the control behavior modeling results, and subsection V.C the human operator and controlled system performance and stability results. The significance of the findings was tested, in most of the cases, using a repeated-measure ANOVA excluding the CPHF condition. Significant effects resulting from this last condition are specifically analyzed in subsection V.D. The SSQ scores are summarized in subsection V.E and the biometrics in subsection V.F.

**Table 2 Means of the aggregated data per simulator type and visual condition.**

Visuals	Simulator	$RMS_e$	$RMS_u$	$K_p$	$T_l$	$\tau$	$\omega_{nm}$	$\zeta_{nm}$	$\omega_c$	$\varphi_m$
C	Fixed-base	1.337	3.551	0.105	2.485	0.363	5.616	0.605	1.053	32.747
CP	Fixed-base	1.451	3.300	0.101	3.086	0.356	5.668	0.635	1.175	32.158
CPHF	Fixed-base	1.339	3.283	0.109	2.510	0.346	5.461	0.565	1.108	32.543
C	VR	1.198	3.310	0.095	2.612	0.349	5.590	0.636	1.025	33.667
CP	VR	1.171	3.040	0.081	3.159	0.334	5.856	0.732	1.035	34.092

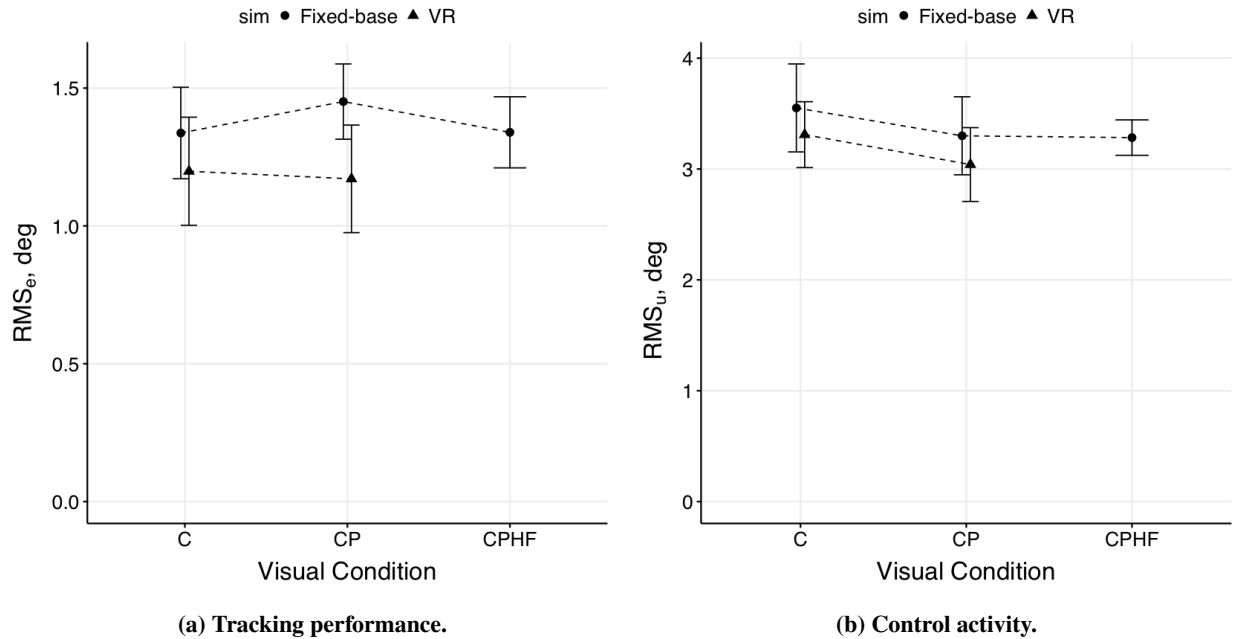
**Table 3 Standard deviations of the aggregated data per simulator type and visual condition.**

Visuals	Simulator	$RMS_e$	$RMS_u$	$K_p$	$T_l$	$\tau$	$\omega_{nm}$	$\zeta_{nm}$	$\omega_c$	$\varphi_m$
C	Fixed-base	0.668	1.219	0.048	0.645	0.050	2.028	0.193	0.292	4.669
CP	Fixed-base	0.685	1.183	0.049	1.129	0.039	2.055	0.206	0.311	6.422
CPHF	Fixed-base	0.547	0.930	0.045	0.700	0.041	1.756	0.166	0.291	5.779
C	VR	0.503	0.962	0.033	0.627	0.025	1.999	0.236	0.214	6.830
CP	VR	0.608	0.880	0.032	1.135	0.029	2.075	0.263	0.320	9.051

**A. Tracking Performance and Control Activity**



Fig. 6 provides the error bar plots of the logarithm of the tracking performance  $RMS_e$  and control activity  $RMS_u$  for all the conditions and simulator types. The bars represent the mean standard error. The statistical analysis was performed on the logarithm of the variables for 2 reasons. Firstly, the residuals of a linear model fitted to the logarithm data were approximately normally distributed while this was not the case for the untransformed data. This allowed us to use a repeated-measure ANOVA. Secondly, reducing the  $RMS_e$  is progressively harder, the lower the score, making it more intuitive to analyze it on a logarithmic scale. The summary of the statistical analysis is provided in Table 4.

The mean  $RMS_e$  in VR ( $M = 1.184$ ) is not significantly different than in the fixed-base simulator setup ( $M = 1.375$ ).

**Fig. 6 Error bar representation of the logarithm of tracking performance and control activity.**

**Table 4 Summary of statistical test results for task performance and control activity.**

Measure	Simulator			Visual Condition			Simulator $\times$ Visual Condition		
	<i>df</i>	<i>F</i>	<i>p</i>	<i>df</i>	<i>F</i>	<i>p</i>	<i>df</i>	<i>F</i>	<i>p</i>
$RMS_e$	1, 11	2.754	0.125	1, 11	0.003	0.954	1, 11	4.305	0.062
$RMS_u$	1, 11	0.798	0.391	1, 11	6.72	0.025	1, 11	0.030	0.865

 = significant ( $p < 0.05$ )  
 = suggestive ( $0.05 < p < 0.1$ )

There was a suggestive interaction between the simulator type and the visual condition type,  $F(1, 11) = 4.305$ ,  $p = 0.062$ . The presence of peripheral visual cues decreased the  $RMS_e$  in VR while this was not the case for the fixed-base simulator. Effect sizes can be deduced from Table 2. The human operator input  $RMS_u$  is significantly affected by the visual condition type,  $F(1, 11) = 6.72$ ,  $p = 0.025$ . The  $RMS_u$  is significantly lower in CP ( $M = 3.170$ ) compared to C ( $M = 3.4305$ ).

### B. Human Operator Control Behavior



The transfer function in Eq. 2 was used to model participants' control behavior in every condition. The five parameters of the transfer function were estimated using MLE with the averaged time series of the error and control inputs over the five measurement runs (Fig. 1) [10]. The optimization problem was solved using the Gauss-Newton method. The MLE procedure was repeated ten times per condition, with different initial conditions for the five parameters each time, to increase the chances of finding a global optimum. Out of the ten solutions, the solution associated with the highest likelihood, and that occurred most frequently, was chosen. Fig. 7 shows an example of a frequency response of the estimated transfer function and the associated Fourier coefficients for one condition of one of the participants.

The estimated human operator models resulting from MLE had an average variance accounted for (VAF) of 71 % for all conditions. In previous research, higher values for the VAF were frequently found as the sample population for the participants was already familiar with the type of control task and their associated performance was higher.

The error bar plots for all the estimated human operator control behavior parameters are provided in Figs. 8 and 9. The bars represent the standard error of the mean. To assess the difference in human operator parameters between the C and CP conditions and the fixed-base simulator and VR setups, we used a repeated-measures ANOVA. The results of the test are summarized in Table 5.

**Table 5 Summary of statistical test results for the human operator parameters.**

Measure	Simulator			Visual Condition			Simulator $\times$ Visual Condition		
	<i>df</i>	<i>F</i>	<i>p</i>	<i>df</i>	<i>F</i>	<i>p</i>	<i>df</i>	<i>F</i>	<i>p</i>
$K_p$	1, 11	1.213	0.294	1, 11	1.410	0.260	1, 11	0.561	0.469
$T_l$	1, 11	0.139	0.716	1, 11	3.711	0.079	1, 11	0.011	0.916
$\tau$	1, 11	4.419	0.059	1, 11	1.526	0.242	1, 11	0.174	0.684
$\omega_{nm}$	1, 11	0.064	0.804	1, 11	0.823	0.139	1, 11	0.176	0.681
$\zeta_{nm}$	1, 11	1.266	0.284	1, 11	1.277	0.282	1, 11	0.417	0.531

 = significant ( $p < 0.05$ )  
 = suggestive ( $0.05 < p < 0.1$ )

The human operator gain  $K_p$  remained approximately constant over all visual conditions both in the fixed-base simulator and in VR (Fig. 8a). Fig. 8b and Table 5 reveal that the lead time constant was suggestively higher in CP ( $M = 3.122$ ) compared to C ( $M = 2.407$ ) in both simulator setups,  $F(1, 11) = 3.711$ ,  $p = 0.079$ . Furthermore the time delay  $\tau$  is suggestively lower in VR ( $M = 0.341$ ) compared to in the fixed-base simulator ( $M = 0.355$ ),  $F(1, 11) = 4.419$ ,  $p = 0.059$ ; however, was approximately constant over all visual conditions (Fig. 9a). The neuromuscular parameters were also approximately constant over all experimental conditions (Figs. 9b and 9c).



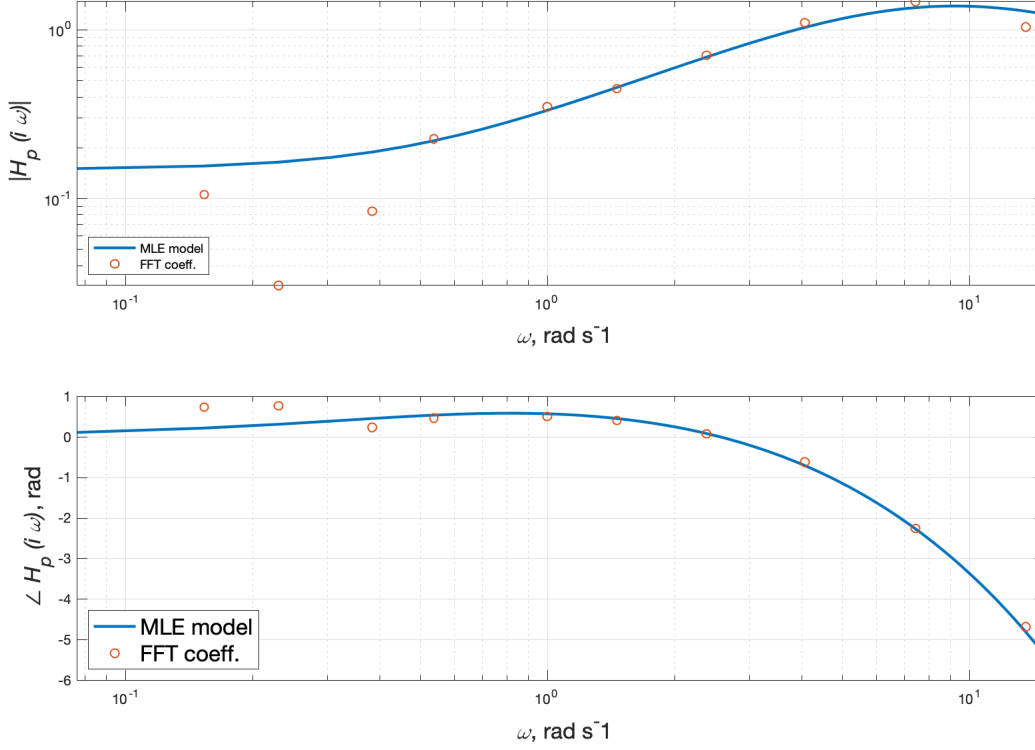


**Fig. 7 Identified human operator model transfer function together with the associated Fourier coefficients for one condition of one participant.**

### C. Open-Loop Parameters

The performance and stability characteristics of the human operator and controlled dynamics were analyzed using the crossover frequency  $\omega_c$  and phase margin  $\varphi_m$  of the open-loop dynamics. Figs. 10a and 10b show the error bar plots for the crossover frequency and phase margin, respectively.

A repeated-measure ANOVA was used to detect significant differences between conditions. The results are summarized in Table 6. The crossover frequency is suggestively higher in CP ( $M = 5.76 \text{ rad s}^{-1}$ ) compared to C ( $M = 5.603 \text{ rad s}^{-1}$ ),  $F(1, 11) = 3.249$ ,  $p = 0.098$ . On the other hand, even though slightly higher in VR, the phase margin seems to be unaffected by the simulator and visual condition type.

**Table 6 Summary of statistical test results for the open-loop parameters.**

Measure	Simulator			Visual condition			Simulator × Visual Condition		
	<i>df</i>	<i>F</i>	<i>p</i>	<i>df</i>	<i>F</i>	<i>p</i>	<i>df</i>	<i>F</i>	<i>p</i>
$\omega_c$	1, 11	1.226	0.284	1, 11	3.249	0.098	1, 11	2.852	0.119
$\varphi_m$	1, 11	1.034	0.331	1, 11	0.004	0.9488	1, 11	0.139	0.716

= significant ( $p < 0.05$ )  
 = suggestive ( $0.05 < p < 0.1$ )

### D. Peripheral Visual Condition

The results from the CPHF condition were compared with the results from the C and CP conditions for the fixed-base simulator only. In the CPHF condition, the checkerboard was positioned further in the peripheral vision, replicating

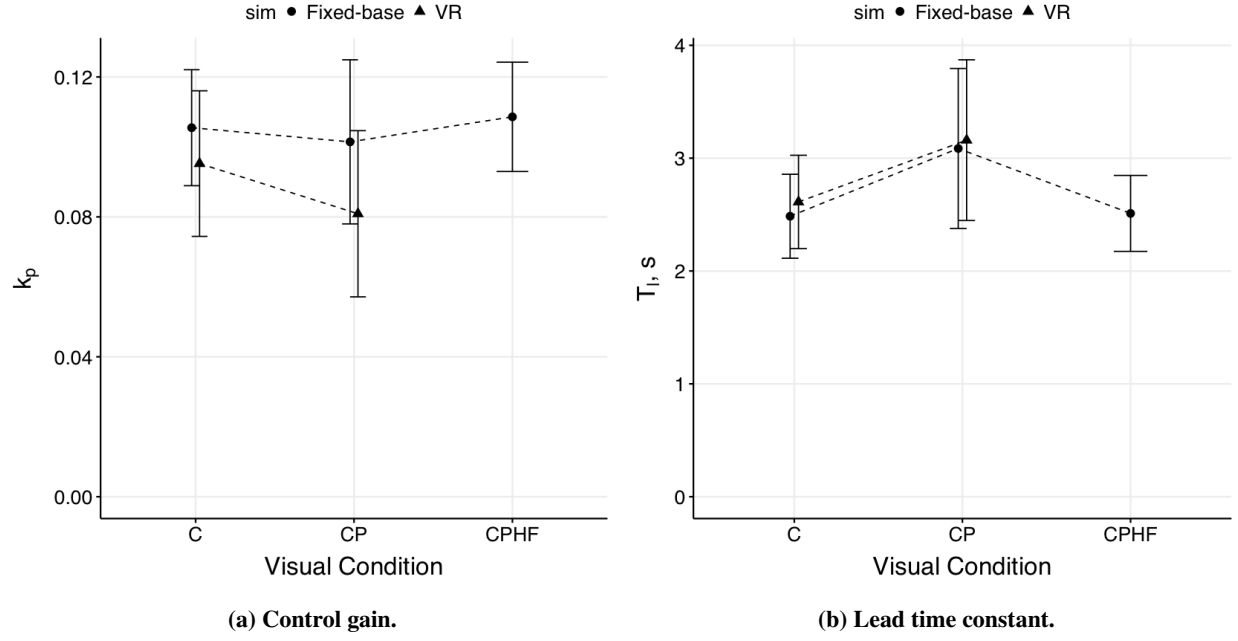


**Fig. 8 Human controller equalization parameters.**

the peripheral visual condition used by Pool et al. [5]. The error bar plots for measured variables and estimated parameters are provided in Figs. 6, 8, 9, and 10.

Since only two conditions were compared and the residuals were approximately normal, a repeated-measures ANOVA was used to detect significant differences in the dependent measures between conditions. In particular, we tested "CP vs CPHF" to see the effects of moving the peripheral visual stimuli closer to the central vision, and "C vs CPHF" to see if we could replicate the trends found by Pool et al. The results of the comparison between the CP and CPHF condition are shown in Table 7, while the results of the comparison between C and CPHF are shown in Table 8.

Tables 7 and 8 reveal that the crossover frequency and lead time constant are significantly or suggestively different between the CP and CPHF conditions only. All other parameters are approximately constant between the visual conditions. The lead time constant  $T_l$  was suggestively higher in CP ( $M = 3.086$ ) compared to in CPHF ( $M = 2.510$ ),  $F(1, 11) = 3.391$ ,  $p = 0.092$ . In addition, the crossover frequency was significantly lower in the CPHF condition ( $M = 1.108$ ,  $\text{rad s}^{-1}$ ) compared to in the CP condition ( $M = 1.174$   $\text{rad s}^{-1}$ ).

**Table 7 ANOVA of CP vs. CPHF.**

Measure	Visual Condition		
	$df$	$F$	p
$RMS_e$	1, 11	1.020	0.330
$RMS_u$	1, 11	0.0371	0.851
$K_p$	1, 11	1.136	0.309
$T_l$	1, 11	3.391	0.092
$\tau$	1, 11	0.681	0.425
$\omega_{nm}$	1, 11	0.649	0.437
$\zeta_{nm}$	1, 11	1.876	0.198
$\omega_c$	1, 11	7.206	0.0212
$\varphi_m$	1, 11	0.079	0.783

**Table 8 ANOVA of C vs. CPHF.**

Measure	Visual Condition		
	$df$	$F$	p
$RMS_e$	1, 11	0.471	0.505
$RMS_u$	1, 11	2.805	0.122
$K_p$	1, 11	0.115	0.740
$T_l$	1, 11	0.0189	0.893
$\tau$	1, 11	2.235	0.163
$\omega_{nm}$	1, 11	0.267	0.615
$\zeta_{nm}$	1, 11	0.539	0.478
$\omega_c$	1, 11	2.595	0.135
$\varphi_m$	1, 11	0.079	0.783

= significant ( $p < 0.05$ )  
 = suggestive ( $0.05 < p < 0.10$ )

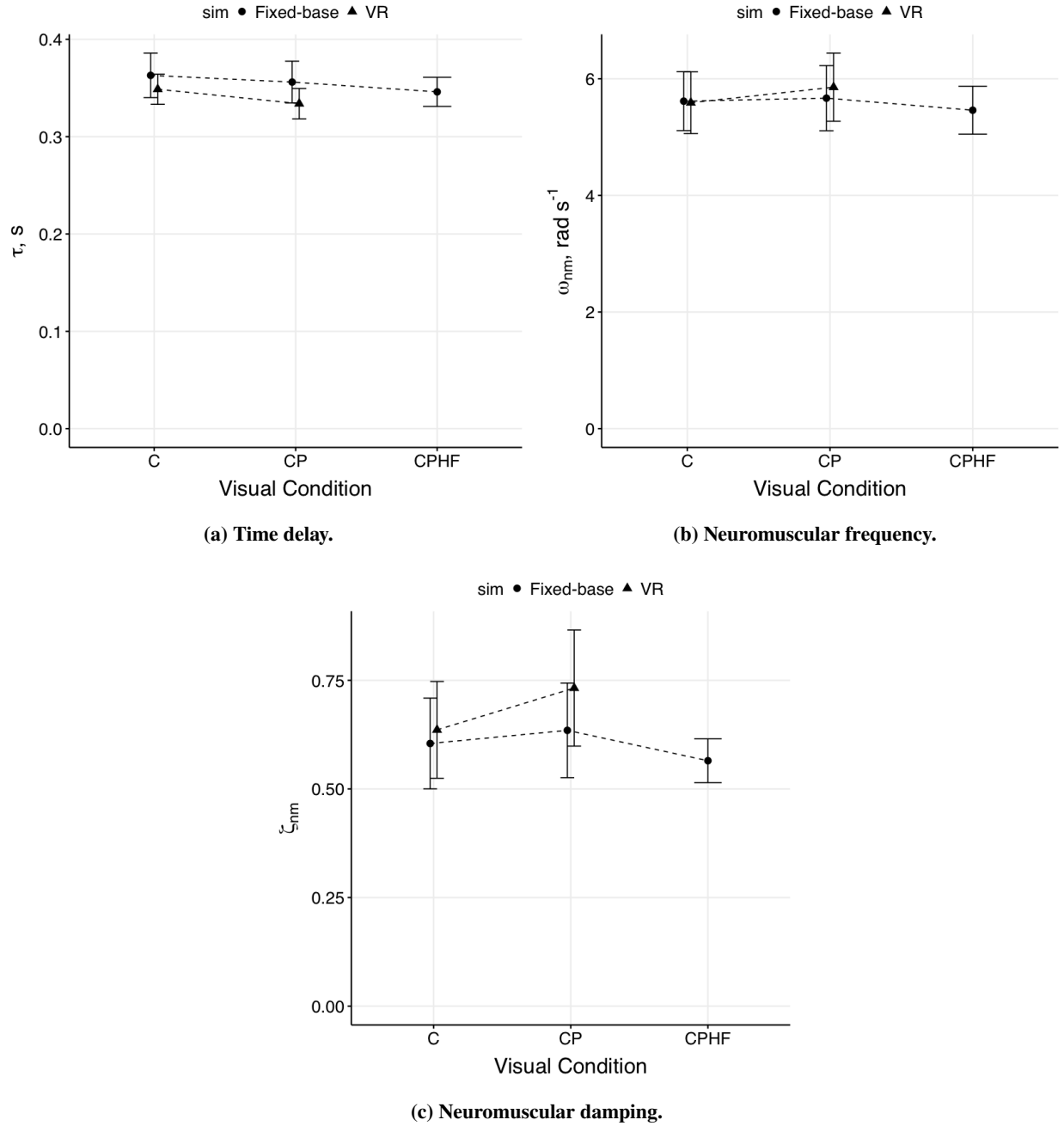


**Fig. 9 Human controller delay and neuromuscular parameters.**

### E. Simulator Sickness Scores

The results of the SSQ were used to assess if VR makes participants more uncomfortable or prone to simulator sickness compared to the conventional fixed-base simulator setup. The total scores were computed by assigning a weight and score to the answer of each question in the SSQ [9]. The symptoms of simulator sickness were clustered in three categories: oculomotor disturbance, nausea, and disorientation.

The scores for the different symptoms for both the conventional simulator and VR are shown in Fig. 11. The total SSQ score for the conventional simulator was 0.93 ( $CI = 1.54$ ) and for VR 6.14 ( $CI = 7.60$ ). Even though SSQ scores in VR were higher compared to the fixed-base simulator, the difference was not significant. The associated symptoms of

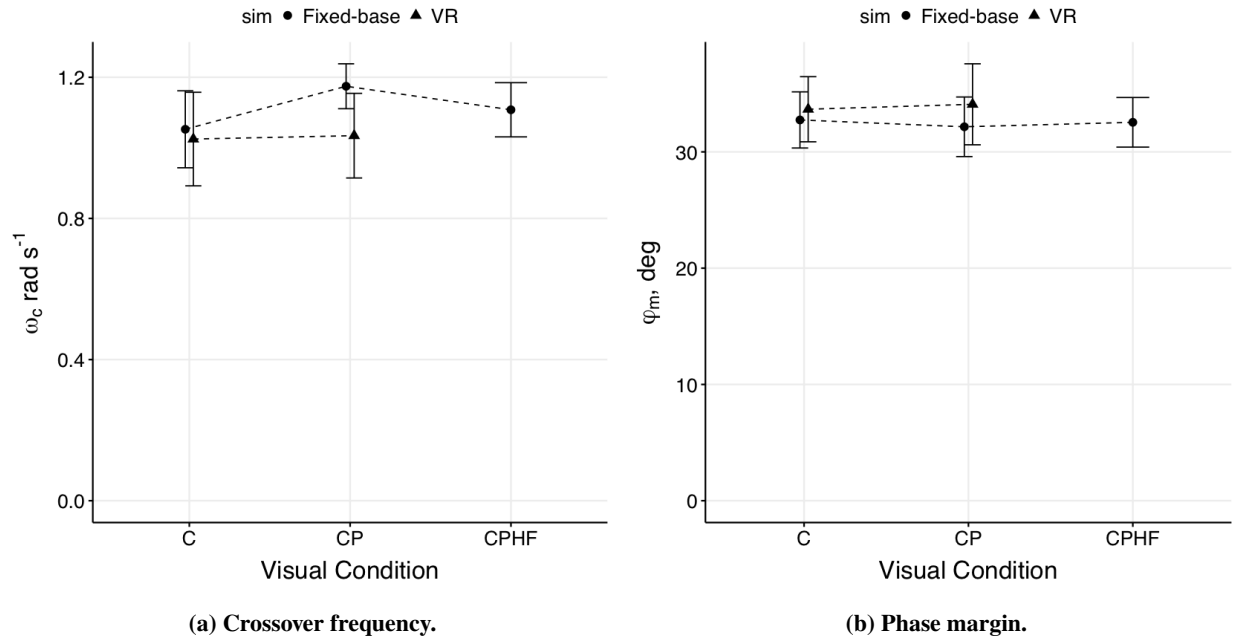


**Fig. 10 Open-loop parameters.**

simulator sickness were very mild in both simulator setups. This result was expected since the visual motion stimuli in both simulators were fairly similar. In VR, the oculomotor symptoms have the highest score. This was expected since participants were looking at close objects for approximately 2 hours in VR.

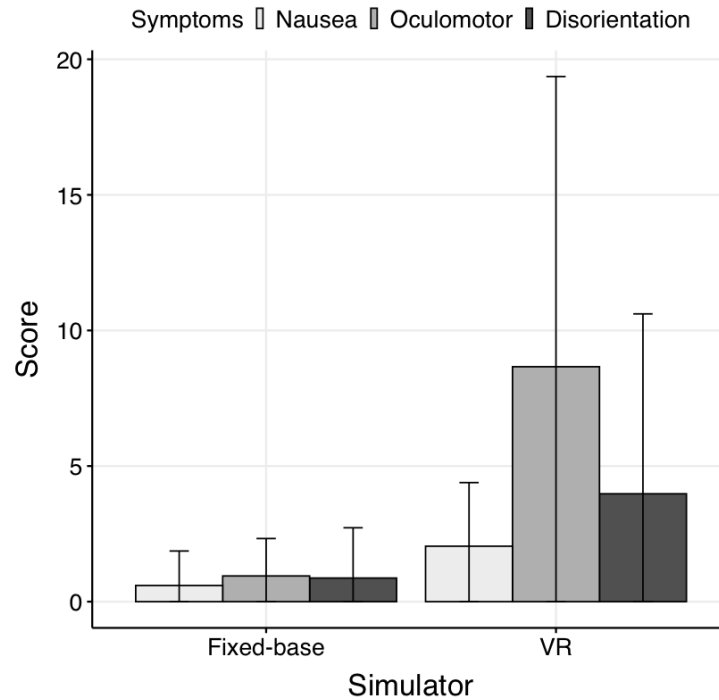


**Fig. 11 SSQ scores subdivided by symptoms for both simulator setups.**

## F. Biometrics

The electrocardiogram (ECG) and skin conductivity (GSC) were measured during every experimental run at a sampling rate of 500 Hz. The measurements were first averaged over a three-second time window. For the statistical analysis the biometrics entries corresponding to the entire length of the run were considered. A mixed-effect model was fit to the data with the simulator type as a fixed effect and the run number nested in the participant identifier as random effects. The ECG and the GSC were not significantly different between the simulator types.

## VI. Discussion

The main purpose of this experiment was to assess whether manual control behavior and performance significantly change in the presence of peripheral visual cues and in a virtual reality environment compared to a conventional fixed-base simulator. The basic experimental setup used in previous studies was utilized in this paper to replicate some of the previous findings and create a baseline. Sec. VI.A addresses the comparison between the fixed-base simulator and VR across the C and CP conditions. Sec. VI.B compares the findings of the current experiment with those from Pool et al. and explains the differences between the CPHF and CP conditions [5].

### A. Simulator and Visual Condition Comparison

The simulator type, i.e., fixed-base or VR, introduced suggestive differences in the tracking performance  $RMS_e$  and the human operator time delay  $\tau$ . Peripheral visual cues only helped to improve tracking performance (reduce  $RMS_e$ ) in VR. This possibly can be attributed to the higher level of immersion of VR compared to conventional simulator visuals allowing users to be more “aware” of the checkerboards patters and their movements. Even though the effect size was small, the human operator delay  $\tau$  was suggestively smaller in VR compared to the fixed-base simulator. This trend could also possibly be attributed to the higher level of engagement and attention that the participants experienced in VR. Visual system delays could also have contributed to the differences found in  $RMS_e$  and  $\tau$ ; however, no attempt was made to measure the different delays of the projection system in the fixed-base simulator setup or of the HMD used in the VR conditions.

Given the observed results we fail to accept hypothesis  $H1$ : participants did not have a lower  $RMS_e$  and lower  $RMS_u$  in the fixed-base simulator compared to VR. Even though the means of both  $RMS_e$  and  $RMS_u$  were lower in VR compared to the fixed-base simulator setup, we cannot reject the null hypothesis for a lack of significant effects. A study with more statistical power could verify this hypothesis.

The visual condition type, i.e., C or CP, introduced significant or suggestive differences in the control effort  $RMS_u$ , lead time constant  $T_l$ , and crossover frequency  $\omega_c$ . In the CP condition, the control effort  $RMS_u$  was significantly lower compared to in the C condition, while the lead constant  $T_l$  and crossover frequency  $\omega_c$  were suggestively higher. These differences, which can also be observed in the error-bar plots, can be attributed to the use of peripheral visual cues in controlling the vehicle dynamics. These peripheral visual cues provide more efficient lead information (roll rate information) resulting in higher human operator lead time constants and consequently higher crossover frequencies. The  $RMS_u$  was lower with peripheral visual cues as participants were most likely more efficient in compensating for the disturbances.

The data lead us to reject hypothesis  $H2$  since the  $RMS_e$  is not significantly different between the C and CP conditions for both simulator types. Also, hypothesis  $H3$  cannot be verified since, even though  $T_l$  is suggestively higher for the CP condition, it is not significantly so.

Interaction effects between the visual condition and the simulator type were mostly absent except for the  $RMS_e$  which showed a suggestive interaction. We fail to reject the null hypothesis related to hypothesis  $H4$  since, even though the presence of the checkerboard patterns seemed to help more in VR, there is not enough evidence to confirm the effect.

The SSQ scores were higher in VR compared to in the fixed-base simulator. In particular the oculomotor disturbance score was higher in VR. Nonetheless, due to the high variability of the scores between participants and the limited dataset we cannot verify hypothesis  $H5$ . VR does not induce significantly more simulator sickness than the conventional visuals in the fixed-base simulator in our experiment.

### B. Replication of Previous Results

The C and CPHF conditions in the fixed-base simulator were exact replicas of the visual conditions used in the study conducted by Pool et al. The CPHF condition replicated the relative positions, sizes and angles between the observer and checkerboard patters from the previous experiment. The CP condition used in the current experiment

had symmetric checkerboards which extended more forward into the visual field due to restrictions imposed by the HMD used for the VR environment. We were interested in understanding if the CP and CPHF conditions provided similar manual control behavior and performance results ( $H6$ ). As can be seen in Table 7, the crossover frequency  $\omega_c$  is significantly different and the lead constant  $T_l$  is suggestively different between CP and CPHF. The remaining measures were not significantly different between the conditions. Therefore we fail to verify  $H6$ , i.e., CP and CPHF did not have an equivalent effect on the dependent measures.

The effect of the peripheral cues was most likely stronger in the CP condition compared to the CPHF condition as a bigger part of the peripheral visual field was covered by the checkerboard pattern as can be seen in Figs. 5a and 5b. The effects found for the CP condition in the current experiment introduced the same trends as in the target-following task or motion conditions, where the peripheral cues or motion had a more significant effect, in the experiment conducted by Pool et al. [5]. A lower control effort  $RMS_u$ , higher lead time constants  $T_l$  and higher crossover frequencies  $\omega_c$  are characteristics that these conditions share compared to the central display only condition.

Comparing C against CPHF, we did not find any significant differences in the dependent measures. This is in line with the findings of the previous experiment conducted by Pool et al., which found that peripheral cues did not introduce significant differences in any of the variables for the easier disturbance-rejection task that was also used in this paper [5]. The absolute values of the dependent measures between the previous and current experiments were not the same since it is notoriously difficult to replicate the exact findings across different simulators due to the many confounding factors [11]. The subject pool, control stick, seat, projectors, and screens were all different in the current experiment compared to the previous experiment. Nonetheless, the trends were replicated between the two experiments.

### C. Biometrics

For each participant we recorded the skin conductivity and the electrocardiogram since they are indicators for motion sickness. In this study, we found that neither of them was correlated with the simulator type (fixed-base simulator or VR). This possibly confirmed the results found with the SSQ that VR did not make participant significantly sicker than the convectional fixed-base simulator. There could be some confounding factors, like the higher level of presence or a different level of the engagement of participants between the two simulator setups.

### D. Limitations and Future Research

This study had some limitations. While VR seemed equally suitable as a fixed-base simulator with conventional visuals for this task, the performance of participants might be lower in VR for a task where a higher resolution of the environment is necessary. Furthermore, the study lacked statistical power as most of the found effects had relatively small effect sizes and therefore the number of participants used was not sufficient to reach significance levels for many trends. It is also unclear if the current findings would apply to pilots as well, who traditionally train on fixed-base simulators and have more flight experience.

This study was a fundamental study to help assess the feasibility of using VR for the training of manual control skills. By finding similar manual control behavior and performance in VR and the fixed-base simulator setup, it was verified that the current VR technology in terms of display resolution and tracking accuracy of the HMD is sufficient for performing manual control tasks. However, more research is required to investigate the effects of the higher immersion that VR provides in more visually realistic environments. Furthermore, it would be useful to investigate the interaction of the VR environment with physical motion cues to assess its effect on human control behavior and cybersickness. This research is necessary to completely validate the use of VR technology for training and other applications in the aerospace industry.

## VII. Conclusion

This paper compared the use of peripheral visual cues in a manual roll disturbance-rejection task between VR and a fixed-base simulator. Furthermore, the experiment aimed to replicate some of the findings of a previous experiment on the effects of peripheral visual cues to allow for a baseline [5]. Fifteen subjects participated in an experiment with two independent variables: the simulator type and the visual condition. In one visual condition, only central visual cues were present on a compensatory display, while in another, peripheral visual cues were added using moving checkerboard patterns. Both these visual conditions were performed in VR and the fixed-base simulator. A third visual condition replicated the peripheral cues from the previous experiment exactly and was only performed in the fixed-base simulator setup.

The results didn't indicate a significant difference in control behavior and performance between VR and the fixed-base simulator. However, there was suggestive evidence that peripheral cues have a stronger effect on improving performance and reducing the human operator visual time delay in VR. This effect could possibly be attributed to the higher level of immersion that VR provides. Peripheral visual cues significantly reduced control effort, increased the human operator lead time constant, and increased the crossover frequency. While the absolute values of the dependent measures were different, the trends found in previous experiments were successfully replicated [4, 5].

By directly comparing manual control behavior and performance between VR and a fixed-base simulator with a conventional visual system, this paper provided data to help determine the validity of using VR for the training of manual control skills. More research is required to compare human control behavior and performance between VR and other training environments to fully understand the benefits and pitfalls of using VR for training.

## VIII. Acknowledgements

The authors would like to thank the fifteen participants who took part in the experiment. In addition, we thank Mike Feary, who allowed us to use the conventional fixed-base simulator and VR equipment of his lab. We also thank Bill Toscano and Fernando Espinosa for their collaboration and help with collecting and processing the biometrics.

## References

- [1] Anthes, C., Garcia-Hernandez, R. J., Wiedemann, M., and Kranzlmuller, D., "State of the Art of Virtual Reality Technology," *2016 IEEE Aerospace Conference*, IEEE, Big Sky, MT, USA, 2016, pp. 1–19. doi:10.1109/aero.2016.7500674.
- [2] Moriarty, T. E., Junker, A. M., and Price, D. R., "Roll Axis Tracking Improvements Resulting from Peripheral Vision Motion Cues," *Twelfth Annual Conference on Manual Control*, 1976, pp. 868–894.
- [3] Hosman, R., and Stassen, H., "Pilot's Perception and Control of Aircraft Motions," *IFAC Proceedings Volumes*, Vol. 31, No. 26, 1998, pp. 311–316. doi:10.1016/s1474-6670(17)40111-x.
- [4] Hosman, R. J. A. W., and van der Vaart, J. C., "Effects of Vestibular and Visual Motion Perception on Task Performance," *Acta Psychologica*, Vol. 48, No. 1-3, 1981, pp. 271–287. doi:10.1016/0001-6918(81)90067-6.
- [5] Pool, D. M., Mulder, M., Van Paassen, M. M., and Van Der Vaart, J. C., "Effects of Peripheral Visual and Physical Motion Cues in Roll-Axis Tracking Tasks," *Journal of Guidance, Control, and Dynamics*, Vol. 31, No. 6, 2008, pp. 1608–1622. doi:10.2514/1.36334.
- [6] Levison, W. H., and Junker, A. M., "A Model for the Pilot's Use of Motion Cues in Roll-Axis Tracking Tasks," Tech. Rep. AMRL-TR-77-40, Bolt Beranek and Newman Inc., Jun. 1977. URL <https://apps.dtic.mil/docs/citations/ADA043690>.
- [7] Meiry, J. L., "The Vestibular System and Human Dynamic Space Orientation," Tech. Rep. NASA CR-628, National Aeronautics and Space Administration, Dec. 1966. URL <https://ntrs.nasa.gov/search.jsp?R=19670001428>.
- [8] McRuer, D. T., and Jex, H. R., "A Review of Quasi-Linear Pilot Models," *IEEE Transactions on Human Factors in Electronics*, Vol. HFE-8, No. 3, 1967, pp. 231–249. doi:10.1109/thfe.1967.234304.
- [9] Kennedy, R. S., Drexler, J. M., Compton, D. E., Stanney, K. M., Lanham, S. W., and Harm, D., "Configural Scoring of Simulator Sickness, Cybersickness and Space Adaptation Syndrome: Similarities and Differences?" 2001. URL <https://ntrs.nasa.gov/search.jsp?R=20100033371>.
- [10] Zaal, P. M. T., Pool, D. M., Chu, Q. P., Paassen, M. M. V., Mulder, M., and Mulder, J. A., "Modeling Human Multimodal Perception and Control Using Genetic Maximum Likelihood Estimation," *Journal of Guidance, Control, and Dynamics*, Vol. 32, No. 4, 2009, pp. 1089–1099. doi:10.2514/1.42843.
- [11] Pieters, M. A., Zaal, P., Pool, D. M., Stroosma, O., and Mulder, M., "A Simulator Comparison Study into the Effects of Motion Filter Order on Pilot Control Behavior," *AIAA Scitech 2019 Forum*, American Institute of Aeronautics and Astronautics, 2019. doi:10.2514/6.2019-0712.